

Fracture toughness in additive manufacturing by selective laser sintering: an overview

Liviu Marşavina  | Dan Ioan Stoia  | Linul Emanoil 

Department of Mechanics and Strength of Materials, Politehnica University Timisoara, Timisoara, Romania

Correspondence

Dan Ioan Stoia, Politehnica University Timisoara, Department of Mechanics and Strength of Materials, Politehnica University Timisoara, Timisoara, Romania.
Email: dan.stoia@upt.ro

Funding information

European Union's Horizon 2020 research and innovation program, Grant/Award Number: 857124

Abstract

This paper presents manufacturing, testing, and computing steps for determining the fracture toughness property of polyamide PA 2200 processed by laser sintering using different process parameters. The design of the samples was conducted according to ASTM D5045-99 and ASTM D5528-01, and the fracture tests consist of four-point bending in symmetric and asymmetric configuration and double cantilever beam test. The process parameters selected as variables were in-plane orientation, spatial orientation, energy density of the process, and induced structural defects. The results provide an extended view regarding the variation of fracture properties when the manufacturing conditions in laser sintering are changed.

KEYWORDS

additive manufacturing, fracture toughness, Mode I, polyamide, selective laser sintering

1 | INTRODUCTION

The additive manufacturing (AM) technologies are relatively new and not yet mature, the mechanical and geometrical properties of the parts being directly affected by the process parameters and the knowledge of the part designer and machine operator.

Selective laser sintering (SLS) is an AM technology where the powder particles are fused together by laser energy in order to produce a three-dimensional (3D) solid body. Phenomena like temperature gradients in powder, particles' electrostatic charge during process, local melting pool size, and shape on one hand and process parameters, design, and arrangement strategy on the other hand are highly influencing the structure and properties of the parts.

Therefore, many researchers focus on establishing the technology–property relation by conducting mechanical tests^{1,2} and structural evaluation³ and assessing the geometrical aspects^{4,5} of the AM parts. SLS is one of the AM technologies that belongs to the powder bed fusion branch. It uses raw material in powder form and a laser source for sintering the particles together. The sinterization process led to a porous structure in the entire volume of the part, which directly influences the mechanical properties. Despite intensive research on fracture mechanics of classical obtained materials,^{5–8} few studies cover the fracture behavior of polyamide processed by SLS.^{9–11}

The paper presents an overview of the authors' work on fracture properties of selectively sintered polyamide (PA2200). Since the fracture properties of AM materials are related to the process parameters, the work highlights the influence of in-plane orientation, spatial orientation, energy density, and structural defects on Mode I and II fracture toughness.

2 | MATERIAL AND METHODS

The AM material used in the study for building the specimens was polyamide PA2200 produced by Electro Optical Systems (EOS) GmbH. This is a multiuse material with relatively high strength and stiffness and good manufacturing resolution. It can be used in a large variety of applications starting from visualization to ready-to-use parts. Its biocompatibility makes it a good candidate for disposable elements in medical field.^{12,13} The physical properties of PA2200 as the manufacturer indicate are grain size $56 \mu\text{m}$ (ISO 13320-11)¹⁴; bulk density 0.45 g/cm^3 (EN ISO 60)¹⁵; melting point $172\text{--}180^\circ\text{C}$ (EN ISO 11357-1).¹⁶

The AM process was conducted on EOS Formiga P100 (EOS GmbH Electro Optical Systems) on 3D samples designed according to ASTM D5045-99 and ASTM D5528-01, respectively.^{17,18} All mechanical tests were conducted on 5-kN Zwick tensile machine followed by data analysis and computation of fracture toughness parameters.^{2,19}

The variables considered in the study (Figure 1) and which are considered to highly influence the fracture toughness are:

- in-plane orientation of samples;
- spatial orientation of samples;
- energy density of the process;
- induced structural defects.

The two types of samples, single edge notched specimen (SENB) and double cantilever beam (DCB), were built according to the orientations that are depicted in Figure 2. Here, the three orientations in XY plane were considered: 0° , 45° , and 90° ; the three in-space orientations are a horizontal position (H) having the front face of the model coincident with the XY plane; a vertical (V_1) orientation having the front face of the model aligned with the YZ plane; and the third spatial orientation, oblique (O), angular aligned at 45° with the XY plane. The DCB samples were built for obtaining the fourth orientation (V_2) that has the manufacturing layers on the same plane like the initial crack plane. The volume where the defects are spread starts in the vicinity of the initial crack tip. Four types of DCB were manufactured: having no defect (0%) and with 0.1%, 0.3%, and 0.5%, respectively. The volume for defect spreading was constant for all samples.^{20–23}

Regarding the energy density used for manufacturing the SENB samples, this was selected at three values: $E_1 = 0.067 \text{ J/mm}^2$, $E_2 = 0.046 \text{ J/mm}^2$, and $E_3 = 0.034 \text{ J/mm}^2$.^{24,25} For DCB design, the highest energy was considered ($E_1 = 0.067 \text{ J/mm}^2$) for all samples.

Relaying on force–displacement curves obtained for all SENB samples, Mode I and II fracture toughness was computed using Equations 1 and 2.²⁶ Here, a is the crack length [mm], σ and τ_0 [MPa] are the normal and shear stresses corresponding to Mode I and II loading (calculated with Equations 3 and 4), and f_I and f_{II} the nondimensional stress intensity factors expressed as ratios between crack length and height of the specimen w .

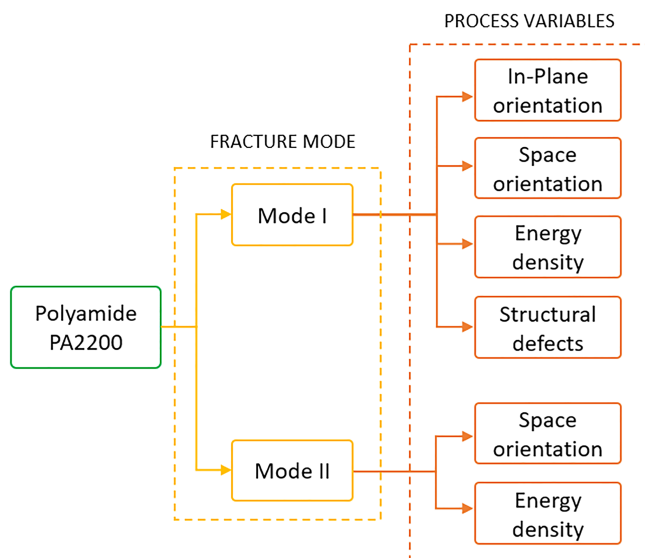


FIGURE 1 The structure of the study

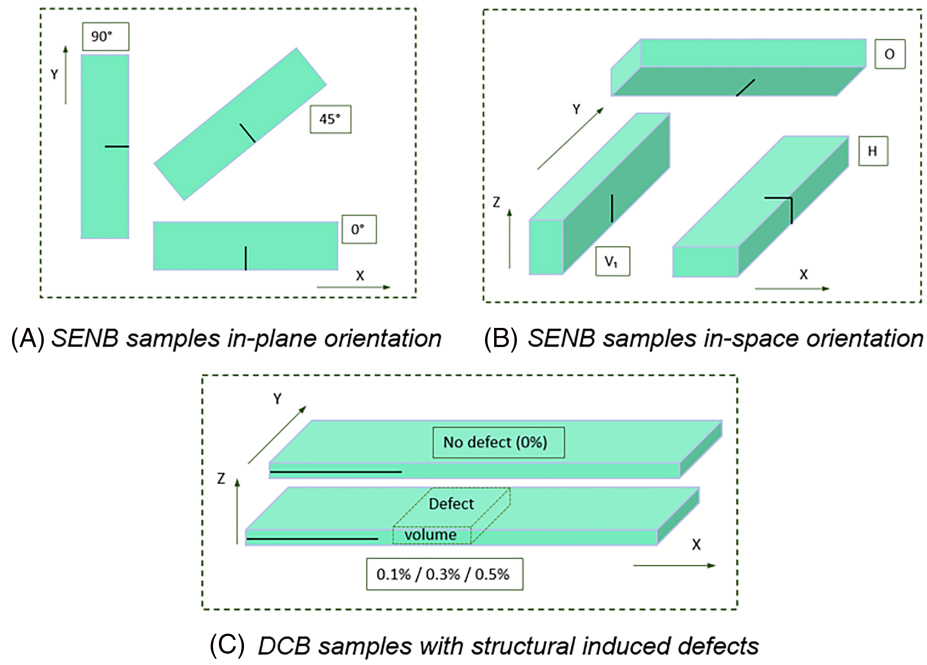


FIGURE 2 Sample types and orientations according to the building envelope

$$K_{IC} = \sigma \sqrt{\pi a} \cdot f_I \left(\frac{a}{w} \right) \quad [MPa \cdot m^{0.5}] \quad (1)$$

$$K_{IIC} = \tau_0 \sqrt{\pi a} \cdot f_{II} \left(\frac{a}{w} \right) \quad [MPa \cdot m^{0.5}] \quad (2)$$

$$\sigma = \frac{3P_Q l}{tW^2} \quad [MPa] \quad (3)$$

$$\tau_0 = \frac{P_Q - Q}{tW} \quad [MPa] \quad (4)$$

In Equations 3 and 4, the terms are as follows: l , distance between the first support and the first loading point; w , specimen height; t , specimen thickness; and P_Q , critical fracture load.

For DCB samples, the critical energy release rate (G_{IC}) was calculated prior to fracture toughness (K_{IC}) using Equations 5 and 6.²⁷ Here, P_{max} is the maximum force, δ is the displacement at P_{max} , b is the sample width, and a_0 initial delamination, $E = 1400$ MPa is Young's modulus, and $\vartheta = 0.41$ is Poisson's ratio of the investigated material.^{2,19}

$$G_{IC} = \frac{3P_{max}\delta}{2ba_0} \quad [N/mm] \quad (5)$$

$$K_{IC} = \sqrt{\frac{G_{IC}E}{1-\vartheta^2}} \quad [MPa \cdot m^{0.5}] \quad (6)$$

3 | RESULTS AND DISCUSSION

The results and discussion are divided into two subsections, one belonging to Mode I fracture and the second one where Mode II fracture is presented. For Mode II, fewer process variables were considered due to the fact that for the first mode, not all the variables significantly influence the fracture toughness.

3.1 | Results of Mode I fracture toughness

Four types of process variables are depicted on abscissa axis, namely, in-plane orientation, in-space orientation, energy density, and structural defects, while on the ordinate is always fracture toughness. This representation type offers a good visualization of process variable—property tendencies (Figures 3–6).

In Figure 3, the effect of in-plane orientation can be observed. This effect of orientation can be put on powder dispenser system and on X–Y directions of the laser scanning system. Due to symmetry in laser scanning for 0° and 90° orientations, the difference of fracture properties for the two positions can be explained by the direction of the powder dispenser travel, related to the orientations. The best fracture toughness was obtained for 0° , which corresponds to an alignment of the long axis of the part with the X axis of the machine (the direction of the velocity vector of powder dispenser).

In spatial conditions, the best properties were obtained for vertical positioning (V_1) of the samples (Figure 4). In this case, the relation between the manufacturing layers and the initial crack is orthogonal, and therefore, by loading the sample on the same direction as the initial crack direction, a pure Mode I will be obtained. On the other hand, when the part grows having the initial crack plane parallel to the manufacturing layers, the fracture properties are poor.

The energy density is a key factor in laser sintering. By mean of this parameter, the material reaches the local temperatures required for sinterization. For this reason, high energy means a better density of the part and therefore a better fracture behavior (Figure 5). The energy–fracture toughness trend is linear and directly proportional, for the highest used energy being recorded values of fracture toughnesses three times higher than for lowest energy value.

Regarding the defect of the structure, here the geometrical positioning of the defect and the defect agglomeration are the main factors of influence (Figure 6). By using a random distribution of defects in a certain volume, the effect of their presence on the fracture toughness is not very clear. However, as the number (percentage) of defects increases, the fracture toughness seems to decrease.

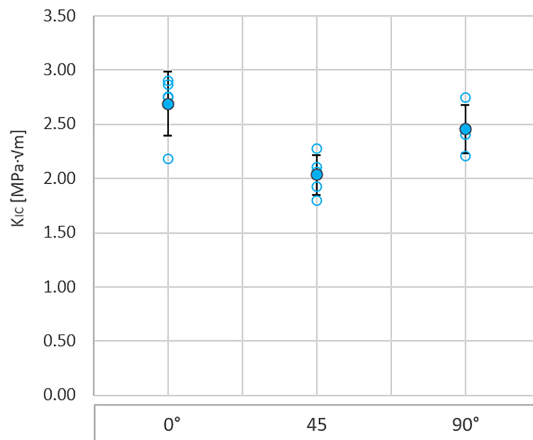


FIGURE 3 Fracture toughness of in-plane oriented samples

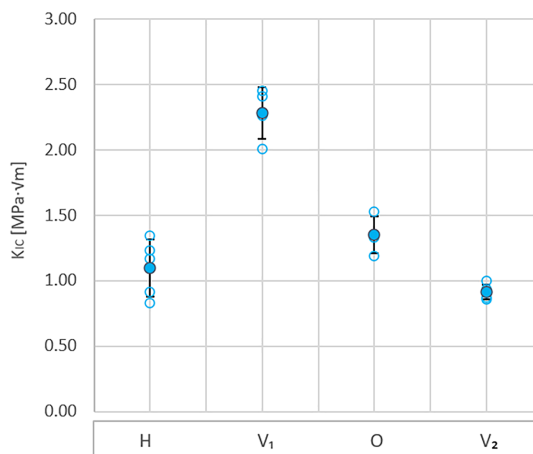


FIGURE 4 Fracture toughness of in-space oriented samples

FIGURE 5 Fracture toughness of samples processed with different energies

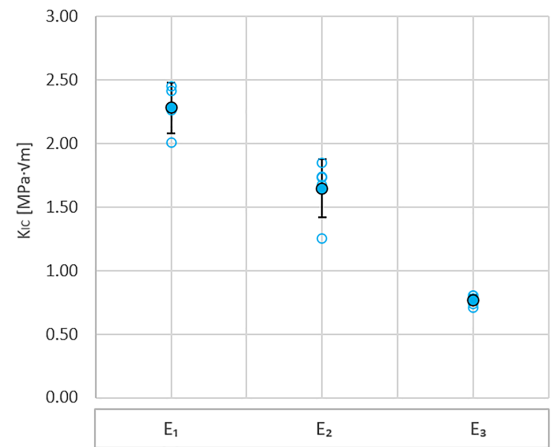


FIGURE 6 Fracture toughness of samples with structural defects

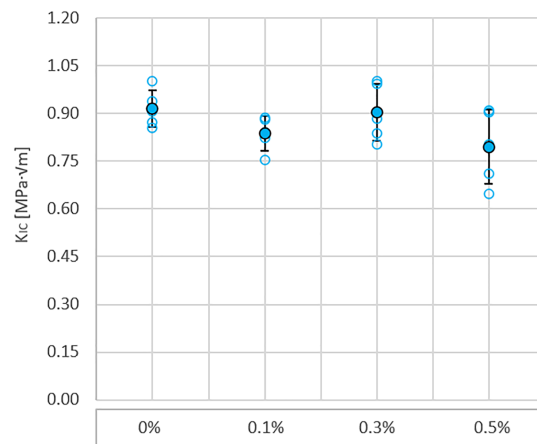
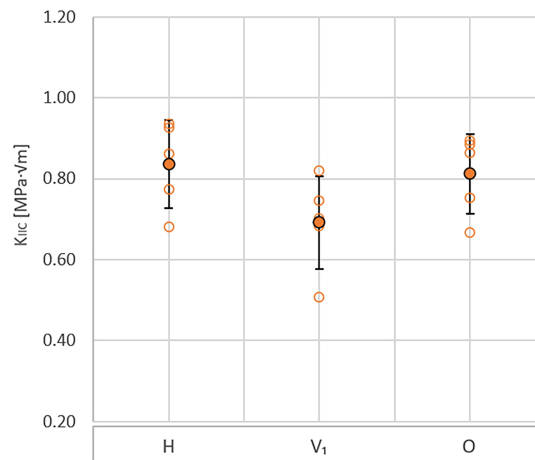


FIGURE 7 Fracture toughness of in-space oriented samples



3.2 | Results of Mode II fracture toughness

Mode II fracture was determined by loading the SENB samples in four-point bending test using an asymmetric configuration. Two process variables were considered for this test: the in-space orientation and the energy density.

The effect of in-space orientation does not follow the same trend for Mode II as for Mode I (Figure 7). The discrete values of fracture toughness are around 2.5 times lower in Mode II. The best value was recorded for horizontal positioning of the sample, when the sample's manufacturing layers and the initial crack plane are perpendicular.

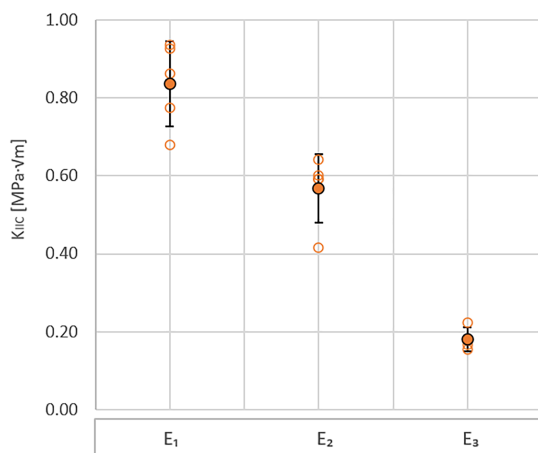


FIGURE 8 Fracture toughness of samples processed with different energies

The influence of the energy density on Mode II (Figure 8) follows exactly the same trend as for Mode I (Figure 5), the discrete values of toughness being 2.6 times lower in this case. This prove that for increasing the density of the part by increasing the value of energy density, the part became less susceptible to fracture propagation, in both Modes I and II.

4 | CONCLUSIONS

The paper presents the authors' work on the fracture toughness of polyamide PA2200 processed by laser sintering. Two different types of samples were used: SENB and DCB for conducting pour-point bending tests in symmetric and asymmetric configurations and DCB test. In processing the samples, four process parameters were used: in-plane orientation, spatial orientation, energy density of the process, and induced structural defects.

By computing the fracture toughness for each individual sample, a significant influence of the process parameters on the fracture properties was identified. Mode I and II fracture toughness was graphically represented according to every individual variable. With slight exceptions, the fracture properties are linearly dependent on density energy and spatial orientation of the sample. Less evident influence was detected for in-plane orientation of samples. Also, as the number of defects in the structure increases, the fracture toughness is more likely to decrease.

ACKNOWLEDGEMENT

The project leading to this application has received funding from the European Union's Horizon 2020 research and innovation program under grant agreement no. 857124.

DATA AVAILABILITY STATEMENT

Raw data were generated at Politehnica University of Timisoara. Derived data supporting the findings of this study are available from the corresponding author (DIS) on request.

ORCID

Liviu Marşavina  <https://orcid.org/0000-0002-5924-0821>

Dan Ioan Stoia  <https://orcid.org/0000-0003-2106-2238>

Linul Emanoil  <https://orcid.org/0000-0001-9090-8917>

REFERENCES

- Griessbach S, Lach R, Grellmann W. Structure–property correlations of laser sintered nylon 12 for dynamic dye testing of plastic parts. *Polym Test*. 2010;29(8):1026-1030.
- Stoia DI, Marşavina L, Linul E. Correlations between process parameters and outcome properties of laser-sintered polyamide. *Polymers*. 2019;11(11):1-15.
- Tan LJ, Zhu W, Sagar K, Zhou K. Comparative study on the selective laser sintering of polypropylene homopolymer and copolymer: processability, crystallization kinetics, crystal phases and mechanical properties. *Addit Manuf*. 2021;37:1-13.

4. Lieneke T, Denzer V, Guido A, Adam O, Zimmer D. Dimensional tolerances for additive manufacturing: experimental investigation for fused deposition modeling. *Procedia CIRP*. 2016;43:286-291.
5. Mousa AA. Experimental investigations of curling phenomenon in selective laser sintering process. *Rapid Prototyping J*. 2006;22:405-415.
6. Aliha MRM, Mousavi SS, Bahmani A, Linul E, Marsavina L. Crack initiation angles and propagation paths in polyurethane foams under mixed modes I/II and I/III loading. *Theor. Appl. Fract. Mech*. 2019;101:152-161.
7. Razavi SMJ, Aliha MRM, Berto F. Application of an average strain energy density criterion to obtain the mixed mode fracture load of granite rock tested with the cracked asymmetric four-point bend specimens. *Theor Appl Fract Mech*. 2017;97:419-425.
8. Ahmed AA, Susmel L. A material length scale-based methodology to assess static strength of notched additively manufactured polylactide (PLA). *Fatig Fract Eng Mater Struct*. 2018;41:2071-2098.
9. Berto MR, Khosravani F, Ayatollahi MR, Reinicke T. Fracture behavior of additively manufactured components: a review. *Theor. Appl. Fract. Mech*. 2020;109:1-14.
10. Crespo M, Gómez-del Río MT, Rodríguez J. Failure of SLS polyamide 12 notched samples at high loading rates. *Theor. Appl. Fract. Mech*. 2017;92:233-239.
11. Young D, Wetmore N, Czabaj M. Interlayer fracture toughness of additively manufactured unreinforced and carbon-fiber-reinforced acrylonitrile butadiene styrene. *Addit Manuf*. 2018;22:508-515.
12. ISO 10993-1. Biological evaluation of medical devices - part 1: evaluation and testing within a risk management process. International Organization for Standardization; 1214 Vernier, Geneva, Switzerland; 2018.
13. EOS GmbH Product information. www.eos.info/material-p (accessed 09 November 2018).
14. ISO 13320. Particle size analysis- laser diffraction methods. International Organization for Standardization, 1214 Vernier, Geneva, Switzerland; 2009.
15. ISO 60. Plastics - determination of apparent density of material that can be poured from a specified funnel. International Organization for Standardization, 1214 Vernier, Geneva, Switzerland; 1977.
16. ISO 11357-1. Plastics - differential scanning calorimetry (DSC) - part 1: general principles. International Organization for Standardization, 1214 Vernier, Geneva, Switzerland; 2016.
17. ASTM D5045-99. Standard test methods for plane-strain fracture toughness and strain energy release rate of plastic materials. <https://www.astm.org/DATABASE>
18. ASTM D5528-01. Standard test method for mode I interlaminar fracture toughness of unidirectional fiber-reinforced polymer matrix composites. ASTM International, West Conshohocken, PA, USA; 2014.
19. Stoia DI, Linul E, Marsavina L. Influence of manufacturing parameters on mechanical properties of porous materials by selective laser sintering. *Materials*. 2019;12(6):1-14.
20. Pilipović A, Valentan B, Šercer M. Influence of SLS processing parameters according to the new mathematical model on flexural properties. *Rapid Prototyping J*. 2016;22(2):258-268.
21. Stoia DI, Marsavina L, Linul E. Mode I fracture toughness of polyamide and alumide samples obtained by selective laser sintering additive process. *Polymers*. 2020;12(3):1-12.
22. Linul E, Marsavina L, Stoia DI. Mode I and II fracture toughness investigation of laser-sintered polyamide. *Theor. Appl. Fract. Mech*. 2020;106:1-11.
23. Stoia DI, Marsavina L, Linul E. Mode I critical energy release rate of additively manufactured polyamide samples. *Theor Appl Fract Mech*. 2021;114:1-10.
24. Pilipović A, Brajljić T, Drstvenšek I. Influence of processing parameters on tensile properties of SLS polymer product. *Polymers*. 2018;10(11):1-18.
25. Marsavina L, Stoia DI. Flexural properties of selectively sintered polyamide and alumide. *Mat Design Process Comm*. 2020;2:1-5.
26. Murakami Y. *Stress Intensity Factors Handbook*. New York: Pergamon Press; 1987.
27. Anderson TL. *Fracture Mechanics: Fundamentals and Applications*. 2nd ed. Boca Raton: CRC Press; 1995.

How to cite this article: Maršavina L, Stoia DI, Emanoil L. Fracture toughness in additive manufacturing by selective laser sintering: an overview. *Mat Design Process Comm*. 2021;3(6):e254. <https://doi.org/10.1002/mdp2.254>

[254](#)